

Aspect-ratio dependence of thermodynamic Casimir forces

Alfred Hucht, Daniel Grüneberg and Felix M. Schmidt
Fakultät für Physik, Universität Duisburg-Essen, D-47048 Duisburg

We consider the three-dimensional Ising model in a $L_{\perp} \times L_{\parallel} \times L_{\parallel}$ cuboid geometry with finite aspect ratio $\rho = L_{\perp}/L_{\parallel}$ and periodic boundary conditions along all directions. For this model the finite-size scaling functions of the excess free energy and thermodynamic Casimir force are evaluated numerically by means of Monte Carlo simulations. The Monte Carlo results compare well with recent field theoretical results for the Ising universality class at temperatures above and slightly below the bulk critical temperature T_c . Furthermore, the excess free energy and Casimir force scaling functions of the two-dimensional Ising model are calculated exactly for arbitrary ρ and compared to the three-dimensional case. We give a general argument that the Casimir force vanishes at the critical point for $\rho = 1$ and becomes repulsive in periodic systems for $\rho > 1$.

I. INTRODUCTION

The spatial confinement of a fluctuating and highly correlated medium may cause long-range forces. The Casimir effect, which was theoretically predicted in 1948 by the Dutch physicist H. B. G. Casimir [1], is a prominent example. This quantum effect is caused by the vacuum fluctuations of the electromagnetic field and has been proven experimentally in the late 1990's [2, 3]. It becomes manifest in an attractive long-range *Casimir force* acting between two parallel, perfectly conducting plates in an electromagnetic vacuum.

Another example for a fluctuation-induced force being of similar nature as the Casimir force in quantum electrodynamics can be found in the physics of critical phenomena [4, 5]. This *thermodynamic Casimir effect* is caused by the spatial confinement of thermal fluctuations near the critical point of a second order phase transition. Experimentally, it has been proven for the first time by measuring the film thickness of superfluid ^4He films as a function of the temperature in the vicinity of the lambda transition [6, 7]. Since then, the thermodynamic Casimir effect was measured in several different systems including binary liquid mixtures [8–10] and tricritical ^3He - ^4He [11].

For several years the shape of the finite-size scaling function determined by Garcia and Chan [6] from the experimental data has not been understood theoretically, in particular its deep minimum right below T_c . While the value of the Casimir force at criticality as well as the decay above T_c could be calculated using field theory [12–15], no quantitative results were available for the scaling region $T \lesssim T_c$ except for mean-field-theoretical approaches [16, 17]. Analytic results exist only for the non-critical region below T_c , where contributions to the thermodynamic Casimir force from Goldstone modes [18–20] and from the excitation of capillary waves of the liquid-vapor ^4He interface [21] become dominant.

This unsatisfactory situation was resolved in Ref. [22], where a method was proposed to calculate the thermodynamic Casimir force for $O(n)$ -symmetrical lattice models using Monte Carlo simulations without any approximations, in contrast to, e. g., the stress tensor method used by Dantchev and Krech [23], which furthermore was re-

stricted to periodic systems. The Monte Carlo simulations were done for the three-dimensional (3D) XY model on a simple cubic lattice with film geometry $L_{\perp} \times L_{\parallel} \times L_{\parallel}$ and open boundary conditions along the \perp -direction, as this system is known to be in the same universality class as the superfluid transition in ^4He and thus displays the same asymptotic critical behavior. The results were found to be in excellent agreement with the experimental results by Garcia, Chan and coworkers [6, 7] and for the first time provided a theoretical explanation for the characteristic shape of the finite-size scaling function and in particular its deep minimum below T_c . In the following, this method was used to determine Casimir forces in various systems and geometries [24, 25], while other methods for the evaluation of thermodynamic Casimir forces using Monte Carlo simulations have also been presented [26–28].

In the present work, this method is used to derive the universal finite-size scaling function of the excess free energy and thermodynamic Casimir force as functions of the aspect ratio $\rho = L_{\perp}/L_{\parallel}$ for the 3D Ising model with cuboid geometry and periodic boundary conditions. Here ρ is allowed to take arbitrary values from $\rho \rightarrow 0$ (film geometry) to $\rho \rightarrow \infty$ (rod geometry), while former investigations were either at $\rho = 0$ [12–17] or limited to the case $\rho \ll 1$ [22–30]. The paper is structured as follows: In the remainder of Sec. I the basic principles and definitions concerning the thermodynamic Casimir effect are discussed and the Monte Carlo method will be revisited. In Sec. II, our Monte Carlo results are discussed and compared to recently published results by Dohm [31] who calculated the Casimir force within a minimal renormalization scheme of the $O(n)$ model at finite ρ , covering temperatures below and above T_c , as well as to field-theoretical results obtained for $T \geq T_c$ in the framework of the renormalization group-improved perturbation theory (RG) to two-loop order [14, 15]. In Sec. III, we present an exact calculation of the excess free energy and Casimir force scaling functions for the two-dimensional (2D) Ising model with arbitrary aspect ratios ρ . We conclude with a discussion and a summary.

A. Basic principles

When a thermodynamical system in d dimensions such as a simple classical fluid or a classical n -vector magnet is confined to a region with thickness L_\perp and cross-sectional area L_\parallel^{d-1} , its total free energy F becomes explicitly size-dependent. Then the reduced free energy per unit volume

$$\begin{aligned} f(T, L_\perp, L_\parallel) &\equiv \frac{F(T, L_\perp, L_\parallel)}{L_\perp L_\parallel^{d-1} k_B T} \\ &= f_\infty(T) + \delta f(T, L_\perp, L_\parallel) \end{aligned} \quad (1)$$

can be decomposed [32] into a sum of the bulk free energy density f_∞ and a finite-size contribution δf . As we assume periodic boundary conditions in all directions, the surface terms in \perp and \parallel directions as well as edge and corner contributions are omitted in (1). In this case the residual free energy δf equals the excess free energy f_{ex} , and we will use f_{ex} instead of δf in the following.

In terms of f_{ex} the reduced thermodynamic Casimir force per surface area in \perp direction is defined as [13]

$$\beta \mathcal{F}_C(T, L_\perp, L_\parallel) \equiv - \frac{\partial [L_\perp f_{\text{ex}}(T, L_\perp, L_\parallel)]}{\partial L_\perp}, \quad (2)$$

where $\beta = 1/k_B T$, and the derivative is taken at fixed L_\parallel . We omit the index \perp for the Casimir force, as we will not consider Casimir forces in parallel directions in this work.

When in the absence of symmetry breaking external fields the critical point is approached from higher temperatures, which corresponds to the liquid-vapor critical point in the case of a simple classical fluid or to the Curie point in a classical n -vector magnet, the bulk correlation length $\xi_\infty(t)$ grows and diverges as [33]

$$\xi_\infty(t) \underset{t>0}{\sim} \xi_+ t^{-\nu}, \quad (3)$$

with correlation length exponent ν , reduced temperature $t = T/T_{c,\infty} - 1$, and non-universal amplitude ξ_+ . In this work we use $\xi_+ = Q_\xi^+ f^+ = 1.000183(2) \times 0.506(1)$ valid for the 3D Ising model on a simple cubic lattice [34, 35].

According to the theory of finite-size scaling [36] and under the assumption, that long-range interactions and other contributions irrelevant in the RG sense are negligible, as for instance subleading long-range interactions [37], the thermodynamic Casimir force in the regime $L_\perp, L_\parallel, \xi_\infty \gg a$, where a is a characteristic microscopic length scale such as the lattice constant in the case of a lattice model, obeys a finite-size scaling form

$$\beta \mathcal{F}_C(T, L_\perp, L_\parallel) \sim L_\perp^{-d} \vartheta_\perp(x_\perp, \rho), \quad (4)$$

where the scaling variable x_\perp can be defined as

$$x_\perp \equiv t \left(\frac{L_\perp}{\xi_+} \right)^{\frac{1}{\nu}} \underset{t>0}{\sim} \left(\frac{L_\perp}{\xi_\infty(t)} \right)^{\frac{1}{\nu}}, \quad (5)$$

$\rho = L_\perp/L_\parallel$ denotes the aspect ratio, and ϑ_\perp is a finite-size scaling function. Note that in this work ϑ always

denotes the scaling function of the Casimir force in \perp direction, while the index describes the reference direction \perp or \parallel of length L .

An analogous finite-size scaling relation holds for the excess free energy,

$$f_{\text{ex}}(T, L_\perp, L_\parallel) \sim L_\perp^{-d} \Theta_\perp(x_\perp, \rho), \quad (6)$$

and ϑ_\perp is related to Θ_\perp according to [31]

$$\vartheta_\perp(x_\perp, \rho) = \left[d - 1 - \frac{1}{\nu} \frac{x_\perp \partial}{\partial x_\perp} - \frac{\rho \partial}{\partial \rho} \right] \Theta_\perp(x_\perp, \rho). \quad (7)$$

The dimensionless finite-size scaling functions Θ_\perp and ϑ_\perp are universal, that is, they only depend on gross properties of the system such as the bulk and surface universality classes of the phase transition, the system shape and boundary conditions, but not on its microscopic details [37, 38].

At the critical point T_c the thermodynamic Casimir force becomes long-ranged and for sufficiently large values of the length L_\perp asymptotically decays as

$$\begin{aligned} \beta \mathcal{F}_C(T_c, L_\perp, L_\parallel) &\sim L_\perp^{-d} \vartheta_\perp(0, \rho) \\ &\sim L_\perp^{-d} [(d-1) \Delta_\perp(\rho) - \rho \Delta'_\perp(\rho)], \end{aligned} \quad (8)$$

where $\Delta_\perp(\rho) \equiv \Theta_\perp(0, \rho)$ is the so-called Casimir amplitude [4], being $-$ like the finite-size scaling function ϑ_\perp – an universal quantity. Note that for finite aspect ratios $\rho > 0$ the Casimir amplitude becomes ρ -dependent. The film geometry is recovered by letting $\rho \rightarrow 0$, and Eq. (8) simplifies to

$$\beta \mathcal{F}_C(T_c, L_\perp, \infty) \sim L_\perp^{-d} (d-1) \Delta_\perp(0). \quad (9)$$

Since the 1990s, such universal quantities have been subject of extensive theoretical research. They were studied by means of exactly solvable models [13, 23, 37, 39–42], Monte Carlo simulations [9, 16, 22–29, 43], as well as within field-theoretical approaches [12–15, 31, 44–46].

B. Reformulation for arbitrary ρ

The formulation of the Casimir force finite-size scaling laws in the previous section was done by assuming film geometry $\rho \ll 1$, i. e., having in mind the limit $\rho \rightarrow 0$. However, if $\rho \gtrsim 1$ this picture is not appropriate and should be replaced by a more general treatment. In the following we rewrite the basic scaling laws in terms of the system volume $V = L_\perp L_\parallel^{d-1}$ instead of the film thickness L_\perp . The resulting scaling functions can be used in the whole regime $0 < \rho < \infty$.

Using the substitution $L_\perp^d \rightarrow V \rho^{d-1}$ in Eq. (6) we get

$$f_{\text{ex}}(T, L_\perp, L_\parallel) \sim V^{-1} \Theta(x, \rho) \quad (10)$$

with an universal scaling function Θ and the generalized scaling variable

$$x \equiv t \left(\frac{V}{\xi_+^d} \right)^{\frac{1}{d\nu}}, \quad (11)$$

while the scaling function Θ_{\perp} from Eq. (6) is recovered as

$$\Theta_{\perp}(x_{\perp}, \rho) = \rho^{d-1} \Theta(x, \rho), \quad (12)$$

with

$$x_{\perp} = \rho^{\frac{1}{\nu} - \frac{1}{d\nu}} x. \quad (13)$$

Similarly, the Casimir force obeys

$$\beta \mathcal{F}_C(T, L_{\perp}, L_{\parallel}) \sim V^{-1} \vartheta(x, \rho), \quad (14)$$

from which we derive the scaling identity

$$\vartheta(x, \rho) = - \left[\frac{1}{d\nu} \frac{x \partial}{\partial x} + \frac{\rho \partial}{\partial \rho} \right] \Theta(x, \rho). \quad (15)$$

Note that this identity is equivalent to but simpler than Eq. (7). At criticality we now define the generalized Casimir amplitude as

$$\Delta(\rho) = \Theta(0, \rho) \quad (16)$$

and find

$$f_{\text{ex}}(T_c, L_{\perp}, L_{\parallel}) \sim V^{-1} \Delta(\rho), \quad (17)$$

$$\beta \mathcal{F}_C(T_c, L_{\perp}, L_{\parallel}) \sim -V^{-1} \rho \Delta'(\rho). \quad (18)$$

The case $\rho = 1$ deserves special attention: As

$$\left. \frac{\partial}{\partial \rho} \Theta(x, \rho) \right|_{\rho=1} = 0 \quad (19)$$

in cubic geometry (see Appendix A), Eq. (15) simplifies to

$$\vartheta(x, 1) = - \frac{1}{d\nu} \frac{x \partial}{\partial x} \Theta(x, 1) \quad (20)$$

at $\rho = 1$, and gives a remarkably simple connection between the Casimir force and the excess internal energy, Eq. (30), in the cube shaped system, namely

$$\beta \mathcal{F}_C(T, L, L) \sim \frac{t}{d\nu} u_{\text{ex}}(T, L, L). \quad (21)$$

Obviously, the Casimir force vanishes at the critical point if $\rho = 1$, i. e.,

$$\vartheta(0, 1) = 0. \quad (22)$$

For completeness we also give the definitions of the scaling functions in terms of L_{\parallel} . As

$$f_{\text{ex}}(T, L_{\perp}, L_{\parallel}) \sim L_{\parallel}^{-d} \Theta_{\parallel}(x_{\parallel}, \rho), \quad (23)$$

we find

$$\Theta_{\parallel}(x_{\parallel}, \rho) = \rho^{-1} \Theta(x, \rho) \quad (24)$$

with $x_{\parallel} \equiv t(L_{\parallel}/\xi_+)^{1/\nu}$. Note that in this representation the scaling identity Eq. (7) reads

$$\vartheta_{\parallel}(x_{\parallel}, \rho) = - \left[1 + \frac{\rho \partial}{\partial \rho} \right] \Theta_{\parallel}(x_{\parallel}, \rho) \quad (25)$$

and in the limit $\rho \rightarrow \infty$ simplifies to

$$\vartheta_{\parallel}(x_{\parallel}, \infty) = -\Theta_{\parallel}(x_{\parallel}, \infty), \quad (26)$$

leading to the simple relation

$$\beta \mathcal{F}_C(T, \infty, L_{\parallel}) \sim -f_{\text{ex}}(T, \infty, L_{\parallel}). \quad (27)$$

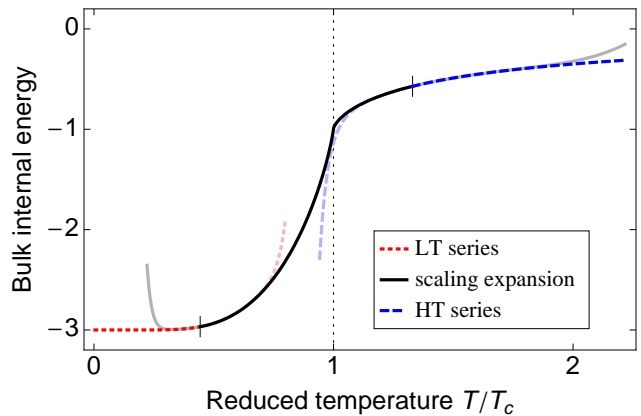


Figure 1. (Color online) Bulk internal energy density $e_{\infty}(T)$ obtained from three different methods: low temperature series [47] (red dotted line), scaling expansion [48] (black line), and high temperature series [49] (blue dashed line).

C. Monte Carlo method

In this work we focus on the three-dimensional isotropic nearest neighbor Ising model on a $L_{\perp} \times L_{\perp} \times L_{\parallel}$ simple cubic lattice with periodic boundary conditions and Hamiltonian

$$\beta \mathcal{H} = - \frac{K}{2} \sum_{\langle ij \rangle} \sigma_i \sigma_j, \quad (28)$$

where $K = \beta J > 0$ is the ferromagnetic reduced exchange interaction and $\sigma_i = \pm 1$ are one-component spin variables at lattice sites i . The Monte Carlo simulations were done using the Wolff single cluster algorithm [50]. Measuring the reduced internal energy density

$$u(T, L_{\perp}, L_{\parallel}) = \frac{\langle \beta \mathcal{H} \rangle}{L_{\parallel}^{d-1} L_{\perp}}, \quad (29)$$

the excess free energy and Casimir force is calculated as follows [22]: First we determined the excess internal energy

$$u_{\text{ex}}(T, L_{\perp}, L_{\parallel}) \equiv u(T, L_{\perp}, L_{\parallel}) - u_{\infty}(T) \quad (30)$$

by subtracting the reduced bulk internal energy density $u_{\infty}(T)$. We used three different results to get precise estimates for $u_{\infty}(T)$ of the $3d$ Ising model in the different temperature regimes: For low temperatures $K > 1/2$ we used the low temperature series expansion (54th order) by Bhanot *et al.* [47], while for $K < 1/6$ the high temperature series expansion (46th order) by Arisue and Fujiwara [49] was utilized. Finally, in the vicinity of the critical point we used the expansion recently obtained by Feng and Blöte [48], where we also took the bulk critical indices [51] $K_c = 0.22165455(3)$, $\nu^{-1} = 1.5868(3)$ and $\omega = 0.821(5)$. These three estimates of $u_{\infty}(T)$ show a broad overlap, see also the discussion by Feng and Blöte

[48], the resulting non-reduced bulk internal energy density $e_\infty(T) = u_\infty(T)/\beta$ is depicted in Fig. 1. With the identity

$$f_{\text{ex}}(T, L_\perp, L_\parallel) = - \int_T^\infty \frac{d\tau}{\tau} u_{\text{ex}}(\tau, L_\perp, L_\parallel) \quad (31)$$

we determined f_{ex} by numerical integration, using the fact that u_{ex} goes exponentially fast to zero above T_c [22].

To obtain the Casimir force, we first calculated the *internal Casimir force*

$$\beta\mathcal{F}_I(T, L_\perp, L_\parallel) = - \frac{\partial[L_\perp u_{\text{ex}}(T, L_\perp, L_\parallel)]}{\partial L_\perp}, \quad (32)$$

which is defined similar to Eq. (2), by numerical differentiation, using thicknesses $L'_\perp = L_\perp \pm 1$ in order to get an integral effective thickness \bar{L}_\perp . With Eqs. (4, 35) and the hyperscaling relation $d\nu = 2 - \alpha$ with specific heat exponent α , it is straightforward to show that this quantity fulfills the finite-size scaling form

$$-\beta\mathcal{F}_I(T, L_\perp, L_\parallel) \sim \xi_+^{-1/\nu} L_\perp^{(\alpha-1)/\nu} \vartheta'_\perp(x_\perp, \rho), \quad (33)$$

with an universal finite-size scaling function

$$\vartheta'_\perp(x_\perp, \rho) = \frac{\partial\vartheta_\perp(x_\perp, \rho)}{\partial x_\perp}. \quad (34)$$

This quantity turns out to be very useful in understanding the Casimir force scaling function $\vartheta_\perp(x_\perp, \rho)$ for $\rho \rightarrow 0$, as will be shown in the next section. Finally, the thermodynamic Casimir force is obtained from Eq. (32) by integration,

$$\beta\mathcal{F}_C(T, L_\perp, L_\parallel) = - \int_T^\infty \frac{d\tau}{\tau} \beta\mathcal{F}_I(\tau, L_\perp, L_\parallel), \quad (35)$$

where again the exponential decay above T_c simplifies the numerical integration.

II. RESULTS

A. Casimir force in film geometry $\rho \rightarrow 0$

In Fig. 2 we plot the internal Casimir force $\beta\mathcal{F}_I$, Eq. (32), for small aspect ratios $\rho = 1/8$ and $\rho = 1/16$. In the limit of film geometry $\rho \rightarrow 0$ we observe strong finite-size effects below the critical point [22], which are caused by the influence of the phase transition in the $d-1$ -dimensional system. In this section we will analyse this influence in detail and show that $\beta\mathcal{F}_I$ is directly connected to the specific heat of the $d-1$ -dimensional system. We will give the derivation for periodic systems where no surface terms occur, as these terms will complicate the analysis [24].

From the scaling identity Eq. (7) for $\rho \rightarrow 0$,

$$\vartheta_\perp(x_\perp, 0) = \left[d - 1 - \frac{1}{\nu} \frac{x_\perp \partial}{\partial x_\perp} \right] \Theta_\perp(x_\perp, 0) \quad (36)$$

we get

$$\beta\mathcal{F}_C \underset{\rho \rightarrow 0}{\sim} (d-1)f_{\text{ex}} + t\nu^{-1}u_{\text{ex}}, \quad (37)$$

i.e., within the scaling region and for $\rho \rightarrow 0$ the Casimir force can alternatively be calculated without L_\perp -derivative [24]. For the internal Casimir force scaling function

$$\vartheta'_\perp(x_\perp, 0) = \left[d - 1 - \frac{1}{\nu} - \frac{1}{\nu} \frac{x_\perp \partial}{\partial x_\perp} \right] \frac{\partial\Theta_\perp(x_\perp, 0)}{\partial x_\perp} \quad (38)$$

we find the asymptotic identity

$$-\beta\mathcal{F}_I \underset{\rho \rightarrow 0}{\sim} - \left[d - 1 - \frac{1-t}{\nu} \right] u_{\text{ex}} + \frac{t}{\nu} c_{\text{ex}} \quad (39)$$

with the excess specific heat

$$c_{\text{ex}}(T, L_\perp, L_\parallel) \equiv c(T, L_\perp, L_\parallel) - c_\infty(T) \quad (40)$$

and $c = \partial Tu / \partial T$ as usual. For $\rho \rightarrow 0$, this quantity contains both the bulk singularity

$$c_\infty(T) \sim A_\pm |t|^{-\alpha}, \quad (41)$$

with amplitudes A_\pm , as well as the singularity of the laterally infinite film with finite thickness L_\perp at $t_c(L_\perp) = T_c(L_\perp)/T_c - 1$, which scales as

$$c(T, L_\perp, \infty) \sim A_\pm^* \left(\frac{L_\perp}{\xi_+} \right)^{\frac{\alpha-\alpha^*}{\nu}} |t - t_c(L_\perp)|^{-\alpha^*}. \quad (42)$$

Here, α^* denotes the specific heat exponent of the $d-1$ -dimensional system, A_\pm^* are amplitudes, and the factor $(L_\perp/\xi_+)^{(\alpha-\alpha^*)/\nu}$ guarantees the correct scaling behavior for $L_\perp \rightarrow \infty$ by cancellation of terms containing α^* .

However, as c_{ex} enters Eq. (39) with prefactor t only, the bulk singularity at $t = 0$ is suppressed (as $\alpha < 1$) and c_{ex} is dominated by the singularity from Eq. (42), at

$$x_\perp^* \sim t_c(L_\perp) \left(\frac{L_\perp}{\xi_+} \right)^{\frac{1}{\nu}}. \quad (43)$$

The location of the critical point was re-analysed from the data of Kitatani *et al.* [52] including corrections to scaling, as well as from the data of Caselle and Hasenbusch [53], giving the value $x_\perp^* = -1.535(10)$. This improves the value $x_\perp^* = -1.60(2)$ found by Vasilyev *et al.* [29]. Furthermore, the other terms in (39) are $O(1)$ near x_\perp^* , which leads us to the conclusion that the specific heat singularity of the $d-1$ -dimensional film is directly visible in the scaling function $\vartheta'_\perp(x_\perp, 0)$ around $x_\perp = x_\perp^*$,

$$\vartheta'_\perp(x_\perp \approx x_\perp^*, 0) \sim \frac{A_\pm^* \xi_+^d}{\nu} x_\perp |x_\perp - x_\perp^*|^{-\alpha^*} + \mathcal{O}(1). \quad (44)$$

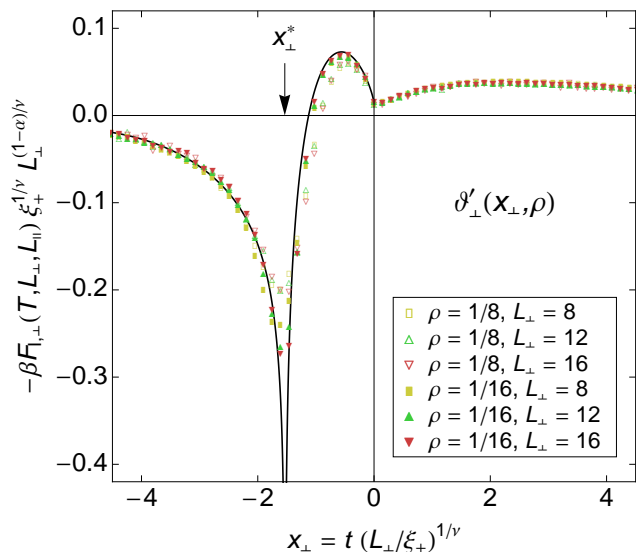


Figure 2. (Color online) Internal Casimir force scaling function $\vartheta'_\perp(x_\perp, \rho)$ for small aspect ratios $\rho = 1/16$ and $\rho = 1/8$. The black thin line is the extrapolation $\rho \rightarrow 0$, showing a logarithmic singularity at $x_\perp^* = 1.535(10)$ (see text).

From this arguments we conclude that the scaling function $\vartheta'_\perp(x_\perp, 0)$ has a singularity at x_\perp^* dominated by the specific heat singularity of the $d-1$ -dimensional system, with critical exponent α^* . In our case, $\alpha^* = 0$ and the singularity is logarithmic. This asymptotic behavior is included in Fig. 2 as solid line.

In Fig. 3 we show the scaling function of the Casimir force for $\rho = 1/8, 1/16$, together with the RG results of Grüneberg and Diehl [15]. The solid line is the integrated extrapolation discussed above. We used a correction factor $(1 + g_1 L_\perp^{-2})$, with $g_1 = -4(1)$, to account for leading systematic errors from the discrete derivative, which are expected to be $\propto L_\perp^{-2}$ in periodic systems. The inset is a magnification of the minimum, from the divergence of $\vartheta'_\perp(x_\perp = x_\perp^*, 0)$ the slope of $\vartheta_\perp(x_\perp, 0)$ at x_\perp^* diverges logarithmically. We find a critical amplitude $\vartheta_\perp(0, 0) = -0.310(6)$ (see Tab. I), which agrees within error bars with the values $\vartheta_\perp(0, 0) = -0.3040(4)$ [29] as well as $\vartheta_\perp(0, 0) = -0.3052(20)$ [54]. The zero at $\vartheta'_\perp(x_\perp^{\min}, 0)$ (solid line in Fig. 2) gives the minimum position $x_\perp^{\min} = -1.13(5)$, with $\vartheta_\perp(x_\perp^{\min}, 0) = -0.360(5)$, while the finite ρ results are $\vartheta_\perp(x_\perp^{\min} = -1.10(5), 1/16) = -0.352(5)$ and $\vartheta_\perp(x_\perp^{\min} = -0.95(5), 1/8) = -0.340(5)$.

B. Casimir force for finite ρ

If we increase ρ to finite values, the Casimir force scaling function $\vartheta_\perp(x_\perp, \rho)$ first changes its shape around the minimum. The results for $\rho = 1/6$ (Fig. 4a) already deviate distinctly from the thinner systems, the minimum below T_c is not so deep anymore, with $\vartheta_\perp(x_\perp^{\min} = -0.77(5), 1/6) = -0.323(5)$. These values deviate only

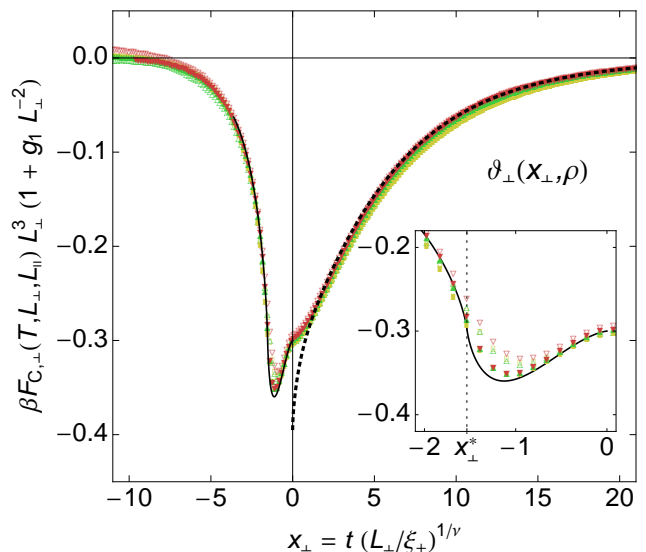


Figure 3. (Color online) Casimir force scaling function $\vartheta_\perp(x_\perp, \rho)$ for small aspect ratios $\rho = 1/16$ and $\rho = 1/8$. The solid line is the extrapolation $\rho \rightarrow 0$ calculated from the integrated logarithmic singularity in $\vartheta'_\perp(x_\perp, 0)$. The dotted line is the RG calculation of Grüneberg and Diehl [15].

slightly from the results of Vasilyev *et al.* [29], $x_\perp^{\min} = -0.681(1)$ and $\vartheta_\perp(x_\perp^{\min}, 1/6) = -0.329(1)$, which we attribute to the larger statistical error in Ref. [29].

When the aspect ratio is further increased to $\rho = 1/4$ (Fig. 4b), the curve has two minima below and above T_c which are nearly equal in depth. Note that the results for $\rho \geq 1/4$ are compared to the predictions of Dohm [31] and show similar behavior. For $\rho \gtrsim 1/4$ the minimum below T_c vanishes, while the one above T_c remains. This is shown in Fig. 4c, where we plot the Casimir scaling function for $\rho = 1/2$.

The results for the cube shaped system with $\rho = 1$ are shown in Fig. 4d [55]. The case $\rho = 1$ is quite interesting, as here the Casimir force at $x = 0$ vanishes (Eq. (22)) and even becomes positive for $\rho > 1$, although the system has symmetric, i. e., periodic boundary conditions. However, this sign change of the Casimir force at $\rho = 1$ does not contradict the predictions of Bachas [56], as he assumed an infinite system in parallel direction, i. e., $\rho = 0$. The scaling function $\vartheta(x, 1)$ has negative slope $\vartheta'(0, 1) = -\Theta'(0, 1)/d\nu$ at $x = 0$. This behavior is in perfect agreement with Eq. (21), as the excess internal energy $u_{\text{ex}}(T_c, L, L)$ is negative for our model. Furthermore, $\vartheta(x, 1)$ has a second zero at $x = -2.25(5)$ where $u(T, L, L) = u_\infty(T)$ holds. Fig. 4d shows results from both the calculation using Eqs. (29-35) (open symbols) as well as Eq. (21) (filled symbols), where the latter have a much better statistics, as no numerical differentiation and integration is necessary.

Finally, in Fig. 5 we depict the Casimir scaling function for values of ρ larger than one. Now we are in rod geometry and use the appropriate scaling variable L_\parallel instead of

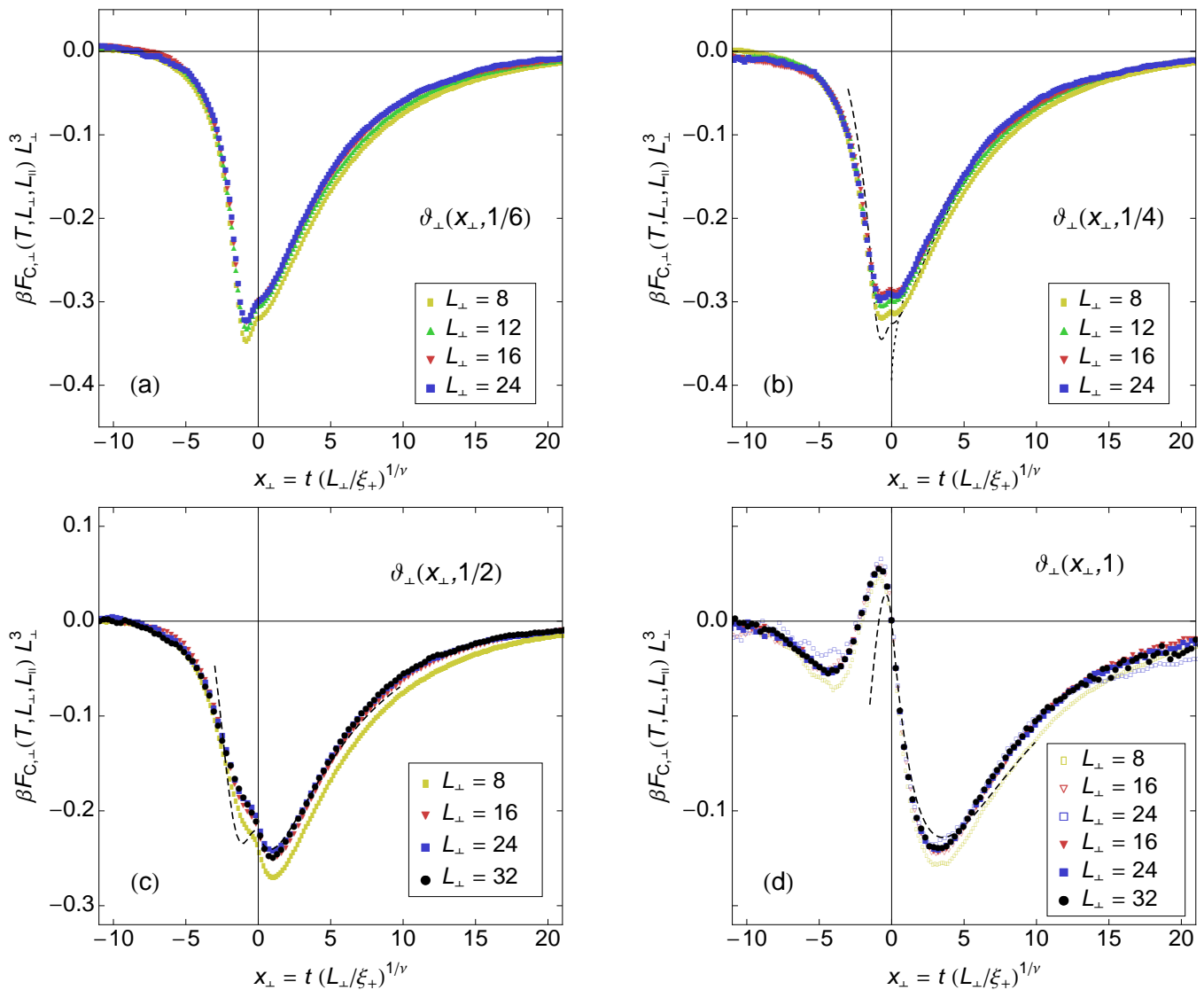


Figure 4. (Color online) Casimir force scaling function $\vartheta_\perp(x_\perp, \rho)$ for several aspect ratios $\rho = \{1/6, 1/4, 1/2, 1\}$. The dotted line is the result of Grüneberg and Diehl [15] for $\rho = 0$, while the dashed lines are the predictions of Dohm [31]. For $\rho = 1$ we also show results from scaling relation Eq. (20) (filled symbols), which have much better statistics, as they are directly calculated from the internal energy.

L_\perp . Due to this rescaling, the scaling function $\vartheta_\parallel(x_\parallel, \rho)$ converges to a finite limit $\vartheta_\parallel(x_\parallel, \infty)$ which should only slightly deviate from curves for $\rho = 8$, just as in the inverse case $\rho = 1/8$ (see Fig. 3). In this regime the Casimir force is always positive, leading to a repulsion of the opposite surfaces. Note that for $\rho = 8$ we increased the thickness difference for the calculation of the derivative in Eq. (32) to $L'_\perp = L_\perp \pm 4$, as, e.g., $L_\perp = 256$ for $L_\parallel = 32$.

C. Excess free energy

The excess free energy is shown in Fig. 6 for $\rho \leq 1$. An interesting feature of these curves is the non-vanishing

limit for $x_\perp \rightarrow -\infty$, which means that for fixed temperatures $T < T_c$ and $L_\perp, L_\parallel \rightarrow \infty$ the total excess free energy Vf_{ex} approaches a finite value. This behavior is a direct consequence of the broken symmetry in the ordered phase [57]: In this phase, which only exists in the thermodynamic limit below T_c , the Ising partition function is reduced by a factor of two, as the system cannot reach the whole phase space anymore. This leads to the term $-\ln 2$ in the total excess free energy of a periodic Ising system below T_c ,

$$\Theta(-\infty, \rho) = -\ln 2, \quad (45)$$

independent of shape and dimensionality. Note that, e.g., for the q -state Potts model this argument directly generalizes to $\Theta(-\infty, \rho) = -\ln q$. Using Eq. (12), we

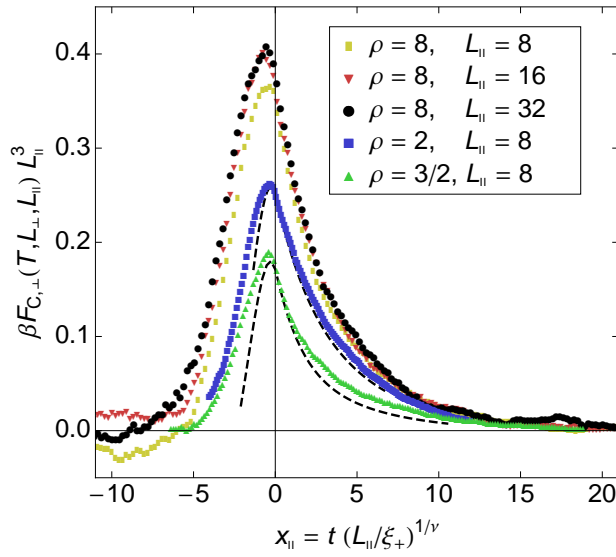


Figure 5. (Color online) Casimir force scaling function $\vartheta_{\parallel}(x_{\parallel}, \rho)$ for aspect ratios $\rho > 1$, now as function of the proper scaling variable x_{\parallel} . The dashed lines are the predictions of Dohm [31].

find

$$\Theta_{\perp}(-\infty, \rho) = -\rho^{d-1} \ln 2, \quad (46)$$

this limit is shown as thin solid lines in Fig. 6. The results are compared to the field theoretical predictions of Dohm [31], we find a satisfactory agreement for positive and also for slightly negative values of x_{\perp} . Furthermore, our value $\Delta(1) = -0.63(1)$ for the cube is compatible with the value $-0.657(30)$ obtained by Mon [58].

The generalized Casimir amplitude at criticality, $\Delta(\rho) = \Theta(0, \rho)$ (Eq. (16)), is listed in Tab. I for several values of ρ and is depicted in Fig. 7, together with the predictions of Dohm [31] (dashed line) as well as the asymptotes (dotted lines). The inset shows $\Delta_{\perp}(\rho)$ (circles) and $\Delta_{\parallel}(1/\rho)$ (squares), showing good agreement with these predictions for $1/4 \lesssim \rho \lesssim 3$.

Table I. Monte Carlo results for the Casimir amplitudes $\Delta(\rho)$, $\Delta_{\mu}(\rho)$ and $\vartheta_{\mu}(0, \rho)$, with $\mu = \perp$ for $\rho \leq 1$ and $\mu = \parallel$ for $\rho \geq 1$. Note that the critical Casimir force changes sign at $\rho = 1$.

ρ	$\Delta(\rho)$	$\Delta_{\mu}(\rho)$	$\vartheta_{\mu}(0, \rho)$
0	$-\infty$	-0.155(3)	-0.310(6)
1/16	-39.8(8)	-0.155(3)	-0.310(6)
1/8	-9.9(2)	-0.155(3)	-0.310(6)
1/6	-5.7(1)	-0.157(3)	-0.30(1)
1/4	-2.60(5)	-0.161(3)	-0.290(5)
1/2	-0.89(2)	-0.223(4)	-0.22(1)
1	-0.63(1)	-0.63(1)	0.000(5)
3/2	-0.68(3)	-0.45(2)	0.17(1)
2	-0.78(3)	-0.39(2)	0.25(1)
8	-2.86(5)	-0.357(8)	0.36(1)
∞	$-\infty$	-0.36(1)	0.36(1)

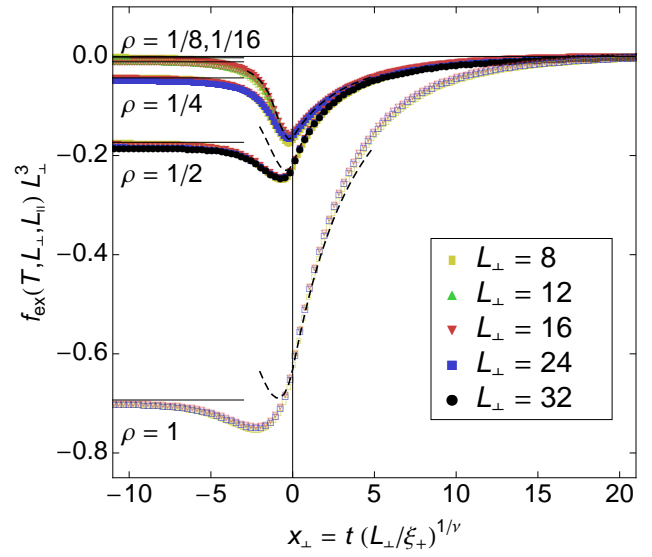


Figure 6. (Color online) Excess free energy scaling function $\Theta_{\perp}(x_{\perp}, \rho)$ for several aspect ratios ρ . The dashed lines are the predictions of Dohm [31] for $\rho = 1/4, 1/2, 1$, while the solid lines are the limits for $x_{\perp} \rightarrow -\infty$, Eq. (46).

III. EXACT RESULTS IN TWO DIMENSIONS

The scaling function Θ_{\perp} of the excess free energy in $d = 2$ is calculated exactly based on the work of Ferdinand and Fisher [59] (Note that the term $\xi S_1(n)\tau^2/2$ is missing in Eq. (3.36) of this work). Our scaling variables

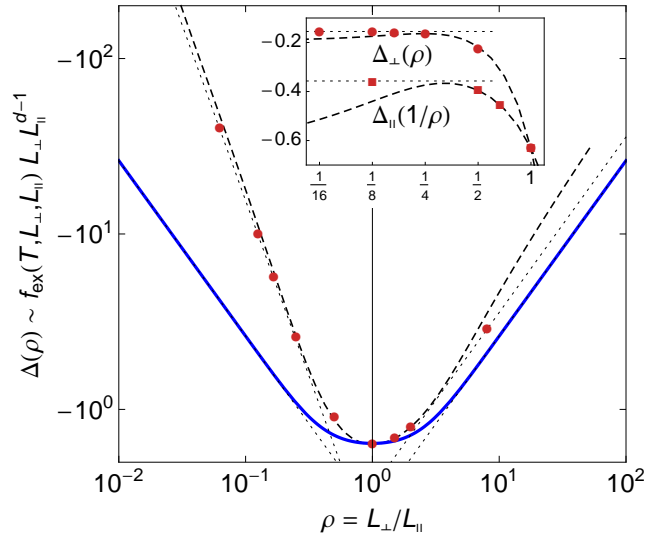


Figure 7. (Color online) Generalized Casimir amplitude $\Delta(\rho) = \Theta(0, \rho)$, Eq. (16), of the Ising universality class in $d = 3$ (red circles, see also Tab. I) and in $d = 2$ (Eq. (56), blue solid line). The dashed line is the prediction of Dohm [31], while the dotted lines show the asymptotes. The inset depicts $\Delta_{\perp}(\rho)$ (circles) and $\Delta_{\parallel}(1/\rho)$ (squares).

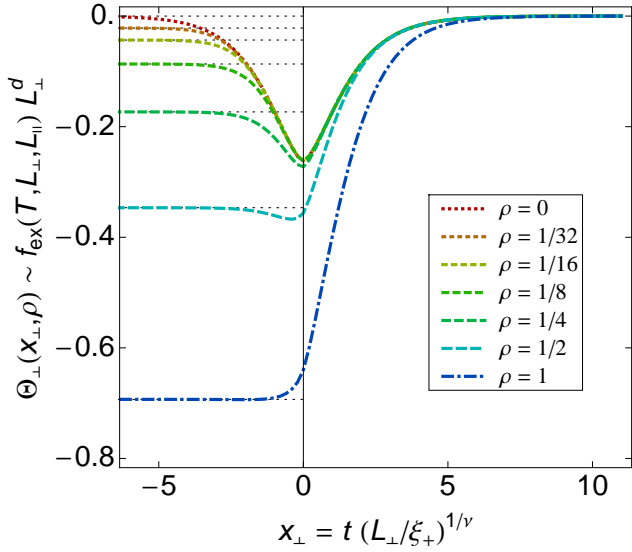


Figure 8. (Color online) Excess free energy scaling function of the $d = 2$ Ising model for several aspect ratios $\rho \leq 1$. The scaling functions for $\rho \geq 1$ can be calculated using Eq. (52).

differ from theirs, we use $x_{\perp} = t(L_{\perp}/\xi_{+})$ and $\rho = L_{\perp}/L_{\parallel}$, while they used $\tau = x_{\perp}/2$ and $\xi = 1/\rho$ as temperature and aspect-ratio variables.

We start from the partition function of the $L_{\perp} \times L_{\parallel}$ isotropic Ising model on a torus [60],

$$Z(T, L_{\perp}, L_{\parallel}) = \frac{1}{2} (2 \sinh 2K)^{\frac{1}{2} L_{\perp} L_{\parallel}} \times (Z_1^+ + Z_1^- + Z_0^+ \pm Z_0^-), \quad (47a)$$

with $+$ above and $-$ below T_c , the four partial sums

$$Z_{\delta}^{\pm} = \prod_{n=0}^{L_{\perp}-1} \left(e^{\frac{1}{2} L_{\parallel} \gamma_{2n+\delta}} \pm e^{\frac{1}{2} L_{\parallel} \gamma_{2n+\delta}} \right), \quad (47b)$$

and $\cosh \gamma_l = \cosh 2K \coth 2K - \cos(l\pi/L_{\perp})$.

For the bulk free energy density of the $d = 2$ Ising model we using *Mathematica* [61] derived a nice closed-form expression not present in the literature yet, namely

$$f_{\infty} = -\ln(2 \cosh 2K) + \frac{k^2}{16} {}_4F_3 \left(\begin{matrix} 1, 1, \frac{3}{2}, \frac{3}{2} \\ 2, 2, 2 \end{matrix} \middle| k^2 \right) \quad (48)$$

with $k = 2 \tanh 2K / \cosh 2K$ and the generalized hypergeometric function ${}_4F_3(\cdot)$ [61].

After some algebra, the scaling function Θ_{\perp} for arbitrary x_{\perp} and ρ can be written as

$$\Theta_{\perp}(x_{\perp}, \rho) = -\rho \ln \left(\frac{P_{1/2}^+ + P_{1/2}^-}{2e^{-I_+/\rho}} + \frac{P_0^+ \pm P_0^-}{2e^{-I_-/\rho}} \right) \quad (49a)$$

with

$$P_{\delta}^{\pm}(x_{\perp}, \rho) = \prod_{n=-\infty}^{\infty} \left(1 \pm e^{-\sqrt{x_{\perp}^2 + 4\pi^2(n-\delta)^2}/\rho} \right) \quad (49b)$$

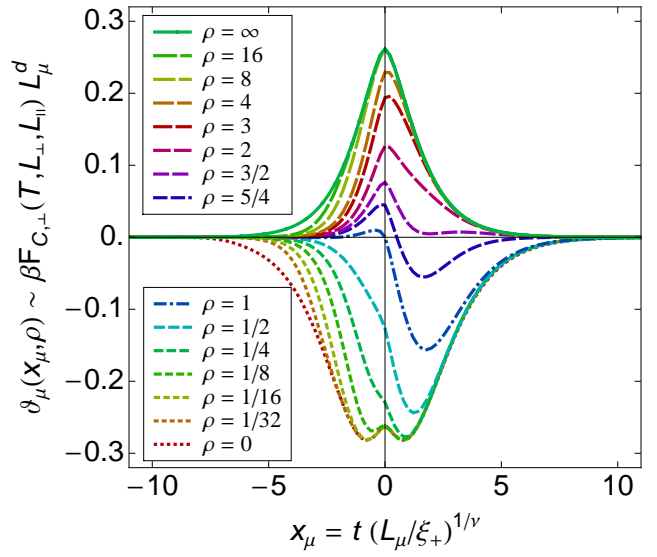


Figure 9. (Color online) Casimir force scaling function $\vartheta_{\mu}(x_{\mu}, \rho)$ of the $d = 2$ Ising model for several aspect ratios ρ . Shown is $\vartheta_{\perp}(x_{\perp}, \rho)$ for $\rho \leq 1$ and $\vartheta_{\parallel}(x_{\parallel}, \rho)$ for $\rho \geq 1$. Note that $\vartheta_{\perp}(x_{\perp}, \rho) = \rho^2 \vartheta_{\parallel}(x_{\parallel}, \rho)$.

and

$$I_{\pm}(x_{\perp}) = \int_{-\infty}^{\infty} d\omega \ln \left(1 \pm e^{-\sqrt{x_{\perp}^2 + 4\pi^2 \omega^2}} \right). \quad (49c)$$

Note that

$$I_{\pm}(x_{\perp}) = \lim_{r \rightarrow \infty} \frac{1}{r} \ln P_{\delta}^{\pm}(rx_{\perp}, r) \quad (50)$$

independent of δ . As the $2d$ system is invariant under exchange of the directions \perp and \parallel ,

$$\Theta(x, \rho) = \Theta(x, 1/\rho), \quad (51)$$

which using Eq. (12) gives

$$\Theta_{\perp}(x_{\perp}, \rho) / \rho = \rho \Theta_{\perp}(x_{\perp} / \rho, 1/\rho), \quad (52)$$

we can derive the identities

$$\frac{P_{1/2}^+(x_{\perp}, \rho)}{P_{1/2}^+(x_{\perp}/\rho, 1/\rho)} = \frac{e^{\rho I_+(x_{\perp}/\rho)}}{e^{I_+(x_{\perp})/\rho}}, \quad (53a)$$

$$\frac{P_{1/2}^-(x_{\perp}, \rho)}{P_0^+(x_{\perp}/\rho, 1/\rho)} = \frac{e^{\rho I_-(x_{\perp}/\rho)}}{e^{I_+(x_{\perp})/\rho}}, \quad (53b)$$

$$\frac{P_0^-(x_{\perp}, \rho)}{P_0^-(x_{\perp}/\rho, 1/\rho)} = \frac{e^{\rho I_-(x_{\perp}/\rho)}}{e^{I_-(x_{\perp})/\rho}}, \quad (53c)$$

which are a generalization of Jacobi's imaginary transformations for elliptic ϑ functions [62].

The resulting excess free energy scaling function $\Theta_{\perp}(x_{\perp}, \rho)$ is depicted in Fig. 8, showing a similar behavior as in the three-dimensional case. For $x_{\perp} \rightarrow -\infty$ Eq. (49) simplifies to

$$\Theta_{\perp}(-\infty, \rho) = -\rho \ln 2, \quad (54)$$

as explained in Sec. II C.

From Eq. (49) we directly obtain values of the scaling function at the critical point $x_{\perp} = 0$, as

$$I_{+}(0) = \frac{\pi}{12}, \quad I_{-}(0) = -\frac{\pi}{6}, \quad (55a)$$

and

$$P_{1/2}^{\pm}(0, \rho) = (\mp q; q^2)_{\infty}^2, \quad P_0^{\pm}(0, \rho) = \frac{1}{2}(\mp 1; q^2)_{\infty}^2 \quad (55b)$$

with $q = e^{-\pi/\rho}$ and the q -Pochhammer symbol [61] $(a; q)_{\infty}$, leading to

$$\begin{aligned} \Theta_{\perp}(0, \rho) &= -\rho \ln \left(\frac{(-q; q^2)_{\infty}^2 + (q; q^2)_{\infty}^2}{2q^{1/12}} + \frac{(-1; q^2)_{\infty}^2}{4q^{-1/6}} \right) \\ &= -\rho \ln \frac{\vartheta_2(0, q) + \vartheta_3(0, q) + \vartheta_4(0, q)}{(4\vartheta_2(0, q)\vartheta_3(0, q)\vartheta_4(0, q))^{1/3}} \end{aligned} \quad (56)$$

after expressing the q -Pochhammer symbols in terms of elliptic ϑ functions. This result was already given by Ferdinand and Fisher [59] (Eq. (3.37)). The resulting Casimir amplitude $\Delta(\rho)$ is shown as blue solid line in Fig. 7.

From the exact solution Eq. (49) we calculated the Casimir force scaling function by numerical differentiation using the scaling relation Eq. (7), as an analytic derivation would be too lengthy for arbitrary ρ . The results are shown in Fig. 9, for $\rho \leq 1$ we show $\vartheta_{\perp}(x_{\perp}, \rho)$, while for $\rho \geq 1$ we show $\vartheta_{\parallel}(x_{\parallel}, \rho)$. Clearly the Casimir force changes sign from negative to positive values with increasing aspect ratio ρ , as in the three-dimensional case.

Finally we give expressions for the limits $\rho \rightarrow 0$ and $\rho \rightarrow \infty$. In film geometry, $\rho \rightarrow 0$, Eq. (49) reduces to the simple result

$$\begin{aligned} \Theta_{\perp}(x_{\perp}, 0) &= -I_{+}(x_{\perp}) \\ &= -\frac{1}{\pi} \int_0^{\infty} d\omega \ln \left(1 + e^{-\sqrt{x_{\perp}^2 + \omega^2}} \right), \end{aligned} \quad (57)$$

yielding the already exactly known Casimir force scaling function [63]

$$\vartheta_{\perp}(x_{\perp}, 0) = -\frac{1}{\pi} \int_0^{\infty} d\omega \frac{\sqrt{x_{\perp}^2 + \omega^2}}{1 + e^{\sqrt{x_{\perp}^2 + \omega^2}}}. \quad (58)$$

In the opposite limit $\rho \rightarrow \infty$ we have

$$\Theta_{\parallel}(x_{\parallel}, \infty) = -\vartheta_{\parallel}(x_{\parallel}, \infty) = -I_{+}(x_{\parallel}) \quad (59)$$

Table II. Signs of the terms $P_{\delta}^{\pm}(x_{\perp}, \rho)$ in Eq. (49a) for different boundary conditions.

BC _⊥	BC _∥	$P_{1/2}^{+}$	$P_{1/2}^{-}$	P_0^{+}	P_0^{-}
periodic	periodic	+	+	+	-
periodic	antiperiodic	+	+	-	+
antiperiodic	periodic	+	-	+	+
antiperiodic	antiperiodic	-	+	+	+

using Eq. (26). For both $\rho \rightarrow 0$ and $\rho \rightarrow \infty$ we have the symmetries $\Theta_{\perp}(x_{\perp}, \rho) = \Theta_{\perp}(-x_{\perp}, \rho)$ and $\vartheta_{\perp}(x_{\perp}, \rho) = \vartheta_{\perp}(-x_{\perp}, \rho)$. Note that all scaling predictions from the previous sections have been verified in the $d = 2$ Ising case. Finally, we remark that these calculations can be easily extended to mixed periodic-antiperiodic boundary conditions by modifying the prefactors of the four terms $P_{\delta}^{\pm}(x_{\perp}, \rho)$ in Eq. (49a) according to Tab. II.

IV. SUMMARY

In this work we calculated the universal excess free energy and Casimir force scaling functions, $\Theta(x, \rho)$ and $\vartheta(x, \rho)$, of the three- and two-dimensional Ising model with arbitrary aspect ratio ρ and periodic boundary conditions in all directions. In $d = 3$ we used Monte Carlo simulations based on the method by Hucht [22], while in $d = 2$ we derived an analytic expression, Eq. (49), for the excess free energy scaling function $\Theta(x, \rho)$. Furthermore, we derived several new scaling identities for the scaling functions: We showed that the Casimir force scaling function $\vartheta_{\perp}(x_{\perp}, 0)$ in the film limit has a singularity of order $(x_{\perp} - x_{\perp}^*)^{1-\alpha^*}$ at the point $x_{\perp}^* < 0$ where the $d-1$ -dimensional system has a phase transition (Eq. (44)), where α^* denotes the specific heat exponent of the $d-1$ -dimensional system. In our case $\alpha^* = 0$ and the singularity is logarithmic as shown in Figs. 2 and 3. At finite values of $\rho \gtrsim 1/4$ our results are compared to field-theoretical results of Dohm, and we find good agreement in the regime $x \gtrsim -2$ where his theory is expected to be valid [31]. For the cube with $\rho = 1$ we observed another interesting result, here the Casimir force vanishes exactly at the critical point, $\vartheta(0, 1) = 0$. In Appendix A this property is shown to hold for all systems that are invariant under permutation of the directions, and is not restricted to periodic systems. The vanishing Casimir force could serve as a stability/instability criterion with respect to ρ : If we assume that the system can change the lengths L_{μ} at constant volume, we see that the cube with $\rho = 1$ and periodic boundary conditions is unstable under variation of ρ at $x = 0$, as $\rho < 1$ tends to $\rho \rightarrow 0$ and $\rho > 1$ tends to $\rho \rightarrow \infty$. Note that this behavior would reverse for antiperiodic boundary conditions, then the cube would be stable at $x = 0$ and the equilibrium shape would even be temperature dependent, as the zero of $\vartheta(x, \rho)$ varies with x , see Fig. 9. For $\rho > 1$ the Casimir force is positive and converges against the negative excess free energy, $\vartheta_{\parallel}(x_{\parallel}, \infty) = -\Theta_{\parallel}(x_{\parallel}, \infty)$, Eq. (26).

The excess free energy below T_c is $f_{\text{ex}} \sim -V^{-1} \ln 2$ in periodic Ising systems [57] independent of system shape (Eq. (45)), leading to a finite ρ -dependent limit of $\Theta_{\perp}(-\infty, \rho)$, Eq. (46).

Finally, the universal scaling function $\Theta_{\perp}(x_{\perp}, \rho)$ is calculated exactly in $d = 2$, and the results are found to be in qualitative agreement with the results for $d = 3$. The most important difference between these two cases is the fact that the $2d$ system has several symmetries

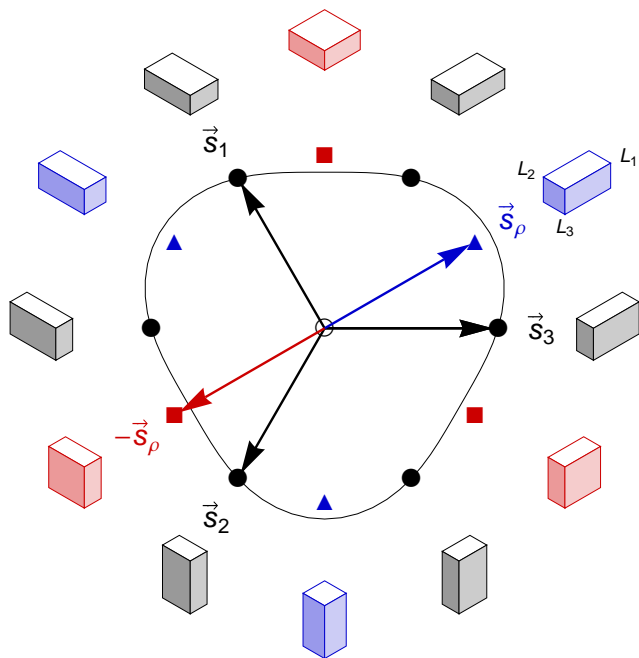


Figure 10. (Color online) The $d-1$ -dimensional plane \mathcal{B} of constant volume L^d for $d=3$, viewed from the normal direction $(1, 1, 1)$. The origin at the center (\circ) is the cube with $\vec{b} = \vec{0}$, while the filled symbols are deformed systems as indicated by the pictures: The black points mark the directions $\pm\vec{s}_\mu$ with constant L_μ symmetric under permutation \mathcal{P} , Eq. (A3). The blue arrow \vec{s}_ρ ($\rho > 1$) and the red arrow $-\vec{s}_\rho$ ($\rho < 1$) mark the direction of the shape variation in terms of ρ used in this work. The black curve sketches a line of constant $\Theta(x, \vec{b})$. Note that $\Theta(x, \vec{s}_\rho) \neq \Theta(x, -\vec{s}_\rho)$, as the shape and thus Θ is not symmetric under the transformation $\rho \rightarrow 1/\rho$, see also Fig. 7.

not present in the $3d$ system, i.e. $(x_\perp, \rho) \leftrightarrow (x_\parallel, 1/\rho)$, $(x, 0) \leftrightarrow (-x, 0)$, and $(x, \infty) \leftrightarrow (-x, \infty)$.

ACKNOWLEDGMENTS

One of the authors (AH) would like to thank Martin Hasenbusch for very useful discussions.

Appendix A: Stationarity of $\Theta(x, \rho)$ at $\rho = 1$

The stationarity of the excess free energy scaling function $\Theta(x, \rho)$ at $\rho = 1$ can be derived for isotropic systems with arbitrary symmetric boundary conditions and in arbitrary dimensions d : We allow arbitrary shape changes of $f_{\text{ex}}(T, L_1, \dots, L_d)$ and write $L_\mu = e^{b_\mu} L$, so that Eq. (10) now reads

$$f_{\text{ex}}(T, e^{b_1} L, \dots, e^{b_d} L) \sim L^{-d} \Theta(x, \vec{b}), \quad (\text{A1})$$

under the condition

$$\sum_{\mu=1}^d b_\mu = 0 \quad (\text{A2})$$

defining the plane \mathcal{B} with constant volume L^d . The symmetry under permutation of the d lattice axes implies

$$\Theta(x, \vec{b}) = \Theta(x, \mathcal{P}(\vec{b})) \quad (\text{A3})$$

with permutation operator \mathcal{P} . This symmetry holds if the boundary conditions in all directions are equal. Without loss of generality we now assume $d=3$, $b_1=0$ and vary the shape of the system along directions 2 and 3, i.e., $b_2 = -b_3$, so that $\Theta(x, \epsilon \vec{s}_1) = \Theta(x, -\epsilon \vec{s}_1)$ with $\vec{s}_1 = (0, 1, -1)$ and real ϵ . Hence $\Theta(x, \epsilon \vec{s}_1)$ is an even function of ϵ and thus the directional derivative along \vec{s}_1 at the origin vanishes,

$$\left. \frac{\partial}{\partial \epsilon} \Theta(x, \epsilon \vec{s}_1) \right|_{\epsilon=0} = 0. \quad (\text{A4})$$

The same argument holds for the symmetric directions $\vec{s}_2 = (-1, 0, 1)$ and $\vec{s}_3 = (1, -1, 0)$ (see Fig. 10). As the $d(d-1)/2$ vectors \vec{s}_μ form an (over)complete base in the $d-1$ -dimensional plane \mathcal{B} , and all directional derivatives vanish at the origin $\vec{b} = \vec{0}$, we conclude that Eq. (A4) holds for all directions $\vec{s} \in \mathcal{B}$. Hence Eq. (A4) also holds for the special case $\vec{s}_\rho = (2/3, -1/3, -1/3)$ which is the direction of the shape variation used in this work (with $\rho = e^\epsilon$), if we set $L_1 = L_\perp$ and $L_2 = L_3 = L_\parallel$. From this we conclude that Eq. (10) satisfies

$$\left. \frac{\partial}{\partial \rho} \Theta(x, \rho) \right|_{\rho=1} = 0. \quad (\text{A5})$$

Note that these arguments can be extended to weakly anisotropic systems, while less is known in the strongly anisotropic case [46, 64].

Appendix B: Proof of $\vartheta(0, 1) = 0$ in the large- n limit

In this appendix we show for the large- n limit [31] that the finite-size scaling function of the thermodynamic Casimir force vanishes at bulk criticality in the case of a cubic system geometry $\rho = 1$. To this end we start from the scaling function of the singular free energy per volume given by Dohm (Eq. (3) in [31]), together with the self-consistency equation for the parameter $P(x_\perp, \rho)$ at $x_\perp = 0$,

$$P(0, \rho) = -4\pi \mathcal{G}_1(P(0, \rho)^2, \rho), \quad (\text{B1})$$

and the functions $\mathcal{G}_j(P^2, \rho)$ (Eq. (4) in [31]). Introducing the parameter $\hat{P}(\rho) \equiv \rho^\mu P(0, \rho)$ and furthermore the integration variable $\hat{z} = \rho^\delta z$ in the integral $\mathcal{G}_0(P^2, \rho)$, the value of the excess free energy scaling function Θ_\perp (see Eq. (6)) at bulk criticality can be cast in the form

$$\Theta_\perp(0, \rho) = \Delta_\perp(\rho) = \rho^2 \Delta(\rho) \quad (\text{B2})$$

upon setting $\mu = -2/3$ and $\delta = 4/3$, where $\Delta(\rho)$ is given by

$$\Delta(\rho) = -\frac{\hat{P}(\rho)^3}{12\pi} + \frac{1}{2} \int_0^\infty \frac{d\hat{z}}{\hat{z}} \exp\left(-\frac{\hat{z}\hat{P}(\rho)^2}{4\pi^2}\right) \times \left[\left(\frac{\pi}{\hat{z}}\right)^{3/2} - K(\rho^{-4/3}\hat{z})K(\rho^{2/3}\hat{z})^2\right]. \quad (\text{B3})$$

According to Eq. (18) one has

$$\vartheta_\perp(x_\perp = 0, \rho = 1) = -\Delta'(1), \quad (\text{B4})$$

where the derivative of $\Delta(\rho)$ with respect to ρ at $\rho = 1$ becomes

$$\Delta'(1) = -\frac{\hat{P}(1)\hat{P}'(1)}{4\pi} \left[\hat{P}(1) + 4\pi\mathcal{G}_1(\hat{P}(1)^2, 1) \right]. \quad (\text{B5})$$

Since $\hat{P}(1) = P(0, 1)$ is the solution to Eq. (B1) at $\rho = 1$, the expression in square brackets vanishes and thus $\Delta'(1) = 0$.

-
- [1] H. B. G. Casimir, Proc. K. Ned. Akad. Wet., **51**, 793 (1948).
- [2] S. K. Lamoreaux, Phys. Rev. Lett., **78**, 5 (1997), Phys. Rev. Lett., **81**, 5475 (1998) (Erratum), arXiv:1007.4276.
- [3] U. Mohideen and A. Roy, Phys. Rev. Lett., **81**, 4549 (1998).
- [4] M. E. Fisher and P.-G. de Gennes, C. R. Acad. Sci. Paris, Ser. B, **287**, 207 (1978).
- [5] A. Gambassi, Journal of Physics: Conference Series, **161**, 012037 (2009).
- [6] R. Garcia and M. H. W. Chan, Phys. Rev. Lett., **83**, 1187 (1999).
- [7] A. Ganshin, S. Scheidemantel, R. Garcia, and M. H. W. Chan, Phys. Rev. Lett., **97**, 075301 (2006).
- [8] M. Fukuto, Y. F. Yano, and P. S. Pershan, Phys. Rev. Lett., **94**, 135702 (2005).
- [9] C. Hertlein, L. Helden, A. Gambassi, S. Dietrich, and C. Bechinger, Nature, **451**, 172 (2008).
- [10] A. Gambassi, A. Maciolek, C. Hertlein, U. Nellen, L. Helden, C. Bechinger, and S. Dietrich, Phys. Rev. E, **80**, 061143 (2009).
- [11] R. Garcia and M. H. W. Chan, Phys. Rev. Lett., **88**, 086101 (2002).
- [12] M. Krech and S. Dietrich, Phys. Rev. A, **46**, 1886 (1992).
- [13] M. Krech, *Casimir Effect in Critical Systems* (World Scientific, Singapore, 1994).
- [14] H. W. Diehl, D. Grüneberg, and M. A. Shpot, Europhys. Lett., **75**, 241 (2006).
- [15] D. Grüneberg and H. W. Diehl, Phys. Rev. B, **77**, 115409 (2008).
- [16] A. Maciolek, A. Gambassi, and S. Dietrich, Phys. Rev. E, **76**, 031124 (2007).
- [17] R. Zandi, A. Shackell, J. Rudnick, M. Kardar, and L. P. Chayes, Phys. Rev. E, **76**, 030601 (2007).
- [18] H. Li and M. Kardar, Phys. Rev. Lett., **67**, 3275 (1991).
- [19] H. Li and M. Kardar, Phys. Rev. A, **46**, 6490 (1992).
- [20] M. Kardar and R. Golestanian, Rev. Mod. Phys., **71**, 1233 (1999).
- [21] R. Zandi, J. Rudnick, and M. Kardar, Phys. Rev. Lett., **93**, 155302 (2004).
- [22] A. Hucht, Phys. Rev. Lett., **99**, 185301 (2007).
- [23] D. Dantchev and M. Krech, Phys. Rev. E, **69**, 046119 (2004).
- [24] M. Hasenbusch, Phys. Rev. B, **81**, 165412 (2010), arXiv:0907.2847.
- [25] M. Hasenbusch, Phys. Rev. B, **82**, 104425 (2010), arXiv:1005.4749.
- [26] O. Vasilyev, A. Gambassi, A. Maciolek, and S. Dietrich, Europhys. Lett., **80**, 60009 (2007).
- [27] M. Hasenbusch, J. Stat. Mech.: Theory Exp., P07031 (2009), arXiv:0905.2096.
- [28] M. Hasenbusch, Phys. Rev. E, **80**, 061120 (2009), arXiv:0908.3582.
- [29] O. Vasilyev, A. Gambassi, A. Maciolek, and S. Dietrich, Phys. Rev. E, **79**, 041142 (2009).
- [30] F. P. Toldin and S. Dietrich, J. Stat. Mech.: Theory Exp., **2010**, P11003 (2010).
- [31] V. Dohm, Europhys. Lett., **86**, 20001 (5pp) (2009).
- [32] V. Privman, in *Finite Size Scaling and Numerical Simulation of Statistical Systems*, edited by V. Privman (World Scientific, Singapore, 1990) Chap. 1.
- [33] Throughout this work, the symbol \sim means “asymptotically equal” in the respective limit, $L_\parallel, L_\perp \rightarrow \infty$, $T \rightarrow T_c$, keeping the scaling variables x and ρ fixed, i. e., $f(L) \sim g(L) \Leftrightarrow \lim_{L \rightarrow \infty} f(L)/g(L) = 1$.
- [34] M. Campostrini, A. Pelissetto, P. Rossi, and E. Vicari, Phys. Rev. E, **60**, 3526 (1999).
- [35] P. Butera and M. Comi, Phys. Rev. B, **65**, 144431 (2002).
- [36] M. E. Fisher, in *Critical Phenomena, Proceedings of the 51st Enrico Fermi Summer School, Varenna, Italy*, edited by M. S. Green (Academic Press, New York, 1971) pp. 73–98.
- [37] D. Dantchev, H. W. Diehl, and D. Grüneberg, Phys. Rev. E, **73**, 016131 (2006).
- [38] D. Grüneberg and A. Hucht, Phys. Rev. E, **69**, 036104 (2004).
- [39] D. M. Danchev, Phys. Rev. E, **58**, 1455 (1998).
- [40] J. G. Brankov, D. M. Dantchev, and N. S. Tonchev, *Theory of Critical Phenomena in Finite-Size Systems – Scaling and Quantum Effects* (World Scientific, Singapore, 2000).
- [41] D. Dantchev, M. Krech, and S. Dietrich, Phys. Rev. E, **67**, 066120 (2003).
- [42] D. Dantchev and D. Grüneberg, Phys. Rev. E, **79**, 041103 (2009).
- [43] M. Krech and D. P. Landau, Phys. Rev. E, **53**, 4414 (1996).
- [44] F. M. Schmidt and H. W. Diehl, Phys. Rev. Lett., **101**, 100601 (2008).
- [45] H. W. Diehl and D. Grüneberg, Nucl. Phys. B, **822**, 517 (2009).
- [46] M. Burgsmüller, H. W. Diehl, and M. A. Shpot, J. Stat. Mech.: Theory Exp., P11020 (2010).

- [47] G. Bhanot, M. Creutz, I. Horvath, J. Lacki, and J. Weckel, Phys. Rev. E, **49**, 2445 (1994).
- [48] X. Feng and H. W. J. Blöte, Phys. Rev. E, **81**, 031103 (2010).
- [49] H. Arisue and T. Fujiwara, Phys. Rev. E, **67**, 066109 (2003), there is a typo in the 42th order term, the correct value appears in arXiv:hep-lat/0209002.
- [50] U. Wolff, Phys. Rev. Lett., **62**, 361 (1989).
- [51] Y. Deng and H. W. J. Blöte, Phys. Rev. E, **68**, 036125 (2003).
- [52] H. Kitatani, M. Ohta, and N. Ito, J. Phys. Soc. Jpn., **65**, 4050 (1996).
- [53] M. Caselle and M. Hasenbusch, Nucl. Phys. B, **470**, 435 (1996), ISSN 0550-3213.
- [54] M. Krech, Phys. Rev. E, **56**, 1642 (1997).
- [55] At $\rho = 1$ all quantities q obey $q = q_{\perp} = q_{\parallel}$.
- [56] C. P. Bachas, J. Phys A: Math. Theor., **40**, 9089 (2007).
- [57] V. Privman and M. E. Fisher, J. Stat. Phys., **33**, 385 (1983).
- [58] K. K. Mon, Phys. Rev. Lett., **54**, 2671 (1985).
- [59] A. E. Ferdinand and M. E. Fisher, Phys. Rev., **185**, 832 (1969), there is a typo in Eq. (3.36), the term $\xi S_1(n)\tau^2/2$ is missing.
- [60] B. Kaufman, Phys. Rev., **76**, 1232 (1949).
- [61] Wolfram Research, Inc., *Mathematica V7.0*, Champaign, Illinois (2008).
- [62] E. T. Whittaker and G. N. Watson, *A Course in Modern Analysis*, 4th ed. (Cambridge University Press, 1990).
- [63] J. Rudnick, R. Zandi, A. Shackell, and D. Abraham, Phys. Rev. E, **82**, 041118 (2010).
- [64] A. Hucht, J. Phys A: Math. Gen., **35**, L481 (2002).